ARKIV FÖR FYSIK Band 19 nr 6

Communicated 9 November 1960 by Erik Hulthén and Kai Siegbahn

Interaction of 560-MeV negative π-mesons with emulsion nuclei

By Å. Frisk, S. Nilsson, B. E. Ronne and W. Schneider

With 13 figures in the text

ABSTRACT

Interactions of 560 MeV negative pions with emulsion nuclei have been investigated. We have found 4454 stars by area scanning. These yield an interaction mean free path of processes including absorption, charge exchange scattering and inelastic scattering of 28 ± 2 cm. Moreover we have analysed 485 stars in detail. The frequency of stars with charged pions is 33 ± 4 % where those with no heavy prong are excluded. The average kinetic energy of pions from stars with one negative pion is 176 ± 20 MeV. A marked correlation exists between the pion energy and the angle of emission. Eight events with two charged pions and ten with one positive pion have been found. A rough estimate gives a fraction of events with charged pion production of 7 ± 4 %.

1. Introduction

The interactions of negative pions in nuclear emulsion with kinetic energies less than 1500 MeV have been investigated in a number of experiments [1–14]. Only two investigations have been performed in the energy region 300 to 1000 MeV, namely, by Blau and Caulton [8] at 500 MeV and by Blau and Oliver [9] at 750 MeV. These two experiments gave a number of results that were difficult to explain, for instance, the angular and energy distributions of the inelastically scattered pions and the lack of correlation between the energy and the angle of emission.

For this reason it was thought to be desirable to investigate the interactions of 560 MeV negative pions, which were available in this laboratory. The investigation also originated from the desire to have a well-determined relation between the average energy of the inelastically scattered pions and the incoming pion energy. This relation is needed in the analysis of antiproton captures in emulsion [15, 16].

The diffraction scattering of negative pions at the same energy in emulsion has been investigated by Barbaro *et al.* [17].

2. Experimental procedure

The negative π-mesons in an early, unseparated antiproton beam were used in this experiment. 120 pellicles of Ilford G5 emulsions, $4'' \times 7'' \times 600\ \mu$m, were exposed in a manner previously described [18]. The momentum of the incoming particles was

720 MeV/c corresponding to a pion kinetic energy of 590 MeV. The average density of light tracks was $9 \times 10^4/\mathrm{cm}^2$. Most of the tracks with minimum ionization were due to pions, but the beam also contained an unknown fraction of muons and electrons.

The stack was area-scanned in three regions, $2 \times 1\ \mathrm{cm}^2$, situated 1, 6 and 16 cm respectively from the edge where the beam entered. Stars with a primary track of minimum ionisation and within $\pm 10°$ with respect to the beam direction were recorded. The scanning was done under 300 times magnification. In the middle region 1.7 cm^3 of emulsion was scanned and at the entrance and far end 1.4 cm^3. The number of interactions found was 1810 (at 1 cm), 1624 (at 6 cm), and 1020 (at 16 cm). The interactions are almost entirely due to π^--mesons and contribution from other particles can be neglected. The total number of pion stars is thus 4454. Of the stars in the middle region 516 were analysed in detail.

3. Determination of the mean free path

The mean free path of the pions was calculated from the attenuation of the pions in the beam. Care was then taken in order to measure in the direction of the beam. The angular distribution in the emulsion plane of the primary pions is shown in

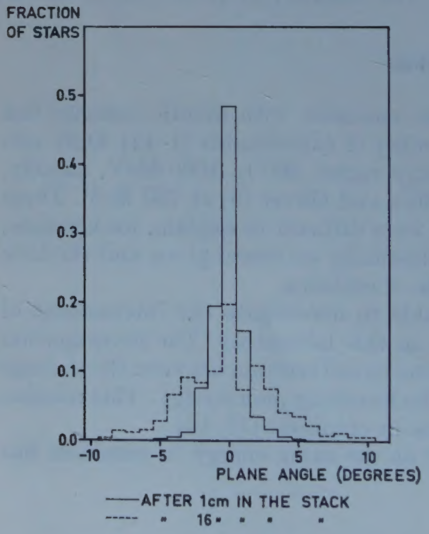

Fig. 1.

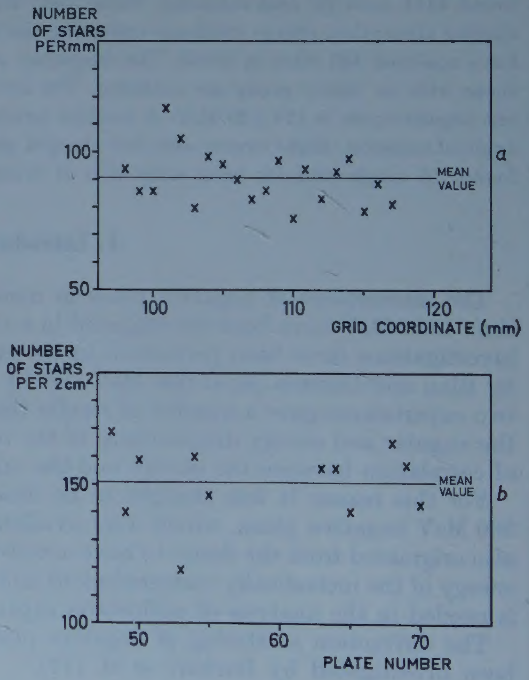

Fig. 2.

Fig. 1. The angular distribution in the emulsion plane of the primary pions after a path length of 1 and 16 cm in the stack.

Fig. 2*a*. The horizontal distribution of stars after a path length of 1 cm. The millimeter grid was numbered from 50 to 150 at the front edge.

Fig. 2*b*. The vertical distribution of stars after a path length of 1 cm.

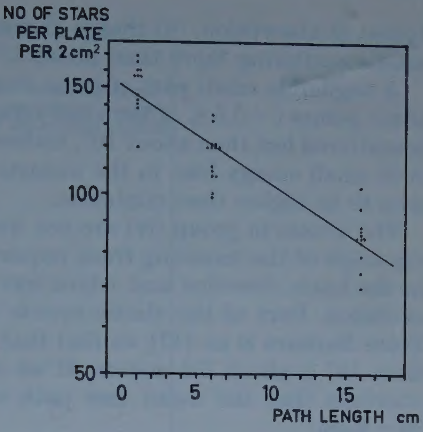

Fig. 3. The attenuation of the pion beam through the stack. The least square line is also shown.

Fig. 1. The angles were measured with respect to a printed coordinate grid on the plates. The diagram shows that the beam direction is a well-defined concept. The distributions in the vertical direction are similar. The standard deviation of the distributions is ± 1.3° at the entrance. In the vertical direction the beam is slightly inclined with respect to the emulsion plane.

The kinetic energy of the pions is 590 MeV at the leading edge and 510 MeV after 16 cm. We assume that the interaction cross-section is constant in this energy interval. Then the number of interactions per unit volume at the three different points will be proportional to the pion flux.

The number of stars for the point at 1 cm from the leading edge is given in Fig. 2*a* and 2*b* for the horizontal (grid coordinate along the front edge of the plate) and vertical (plate number) directions respectively.

The figures show that the flux is homogeneous over the measured area.

The attenuation of the beam through the stack is given in Fig. 3. The number of stars per plate and 2 cm² is plotted as a function of the distance in the stack. The least square line fitted to the points is also shown. One obtains from the figure an interaction mean free path of $\lambda = 27 \pm 2$ cm.

It should be noted that this determination of the mean free path is not affected by scanning bias, provided that the scanners record the same type of events at the different positions and provided that the appearance of the stars does not change with energy in the region 510–590 MeV. The mean free paths obtained by different scanners agree extremely well. The change of the percentage of stars with zero or one black prong, which are the stars likely to be missed, is negligible in the energy interval. Our determination of the mean free path is further independent of the contamination of muons and electrons in the beam.

Another factor which could influence the measurement is multiple Coulomb scattering. A formula derived by Fermi [19] gives that a Dirac δ-distribution of the actual pion energy will be Gaussian with a standard deviation of 4 mm after 15 cm in emulsion. If we leave out stars situated less than 4 mm from any side of the measured area facing the beam, we get $\lambda = 28 \pm 3$ cm, which is in good agreement with the value above. This shows that there are no edge effects arising from inhomogeneities in the flux outside the measured area.

The measured attenuation of the beam is due to interactions of the following types: (i) absorption, (ii) charge-exchange scattering, (iii) inelastic scattering and (iv) elastic scattering more than about 10°.

A negligible small part of pions from group (iii) will, however, be recorded at the three points ($< 0.5\,\%$ of the total number of stars). These are events where the pion is scattered less than about 10°, makes a star in the scanned volume, and has suffered such small energy loss, in the inelastic scattering, that the ionization is not visually seen to be higher than minimum.

The events in group (iv) are not well defined. The pick-up criterion with plane or dip angle of the incoming track required to be $\leqslant 10°$ means that all events originally in the beam direction and which have been scattered an angle $> 14°$ are definitely excluded. Part of the elastic events with space angle 10° to 14° will be recorded. From Barbaro *et al.* [17] we find that the mean free path for elastic scattering more than 10° is about 4.6 meters. If we eliminate the influence of elastic scattering, we conclude that the mean free path of interactions belonging to groups (i)–(iii) is 28 ± 2 cm.

4. Measurements on the emitted particles

4.1 *Identification of the tracks*

Of the 1624 stars in the middle part of the stack 516 have been analysed in detail. Those situated less than 30 μm (unprocessed emulsion) from either surface or glass had a lower charged pion multiplicity (0.22) than the rest of the stars (0.30). This effect is to be expected, owing to experimental loss of tracks with low ionization near surface or glass. Therefore only stars situated more than 30 μm from either surface or glass are included in the following analysis. This number of stars is 485.

The secondary tracks were divided into two groups with relative ionization $g/g_0 \geqslant 1.4$ and $g/g_0 < 1.4$ respectively, where g_0 is the ionization of the pions in the beam.

The first group contains tracks with $g/g_0 \geqslant 1.4$ corresponding to energies of less than 70 MeV (pions) or less than 450 MeV (protons). Prongs shorter than 5 μm are not included in the heavy prong statistics. All tracks with $g/g_0 \geqslant 1.4$ (2297) were followed until the particles were brought to rest in the stack (96.2 %), left the stack (2.5 %) or interacted in flight (1.3 %). The identification of these particles is given in Table 1.

Table 1. The identification of secondary particles with $g/g_0 \geqslant 1.4$.

Particles identified as	Total number of prongs		
	stopping in the stack	leaving the stack	interacting in flight
'protons'	2154	56	26
π-mesons	55	2	4

The masses of the particles which came to rest were in most cases easily obtained from grain density and/or multiple scattering measurements. All tracks with range less than 1 cm which by appearance (decay, interaction, scattering) did not appear

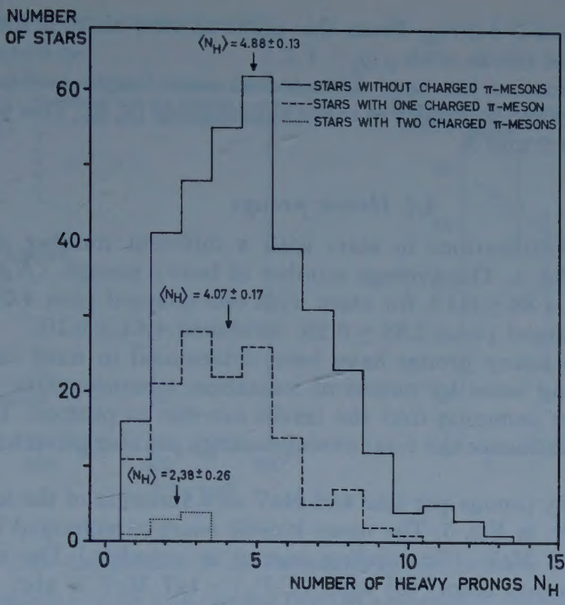

Fig. 4. The experimental heavy prong distributions from the pion stars.

to be due to pions were assumed to be due to 'protons'. The 'protons' in Table 1 include all charged particles heavier than the pion.

The number of particles leaving the stack was 58. The mean range followed per track was 52 mm and no particle left the stack with an observed range less than 30 mm. It was therefore no difficulty to distinguish between pions and protons.

The identity of the 30 particles which interacted in flight was established by a suitable combination of range, grain density, and multiple scattering measurements. In most cases the identification is beyond any doubt.

In the second ionization group with $g/g_0 < 1.4$ there are 92 tracks. Careful mass determinations by a combination of grain density and multiple scattering measurements have been performed on about half of this number of tracks. All measured tracks were consistent with pion tracks. All tracks in this group are therefore taken as pions.

In the following some auxiliary consistency checks are discussed. The percentage of π_0 (stars at rest without secondary charged particles) among the stopping π^--mesons is 21 ± 7 % which is in good agreement with other experiments [20, 21]. In a pion track length of 1.25 m, four interactions in flight were found. This is also reasonable if one assumes a geometrical mean free path. Further, about 14 m of proton tracks have been followed, in which 26 interactions were found, i.e. the mean free path is 53 ± 10 cm. In the antiproton experiment [16] the energy spectrum of the heavy prongs was about the same (Fig. 5) as in this pion experiment. There a mean free path of 49 ± 9 cm was obtained. The good agreement confirms that the particle identification in this experiment is essentially correct.

Furthermore, by kinematic considerations, a proton can only reach a maximum energy of about 510 MeV (assuming a Fermi energy of the nucleon of 33 MeV). The corresponding ionization is 1.30 g_0. From this point of view there is likely to be few protons in the group of tracks with $g/g_0 < 1.4$.

The particle identification has been discussed at some length because our results differ in some points from the results of other experiments [8, 9]. This will be further discussed in sections 4.2 and 5.

4.2 *Heavy prongs*

The heavy prong distributions in stars with a different number of charged π-mesons are given in Fig. 4. The average number of heavy prongs, $\langle N_H \rangle$, is for stars without charged pion 4.88 ± 0.13, for stars with one charged pion 4.07 ± 0.17, and for stars with two charged pions 2.38 ± 0.26, combined 4.61 ± 0.10.

The energies of the heavy prongs have been determined in most cases from the range, in the remaining cases by means of ionization measurements. The energies have been obtained by assuming that the tracks are due to protons. This does not, however, appreciably influence the total average energy per star given to the evaporation prongs.

The number of heavy prongs per star and MeV as a function of the kinetic energy of the particle is shown in Fig. 5. The mean kinetic energy in charged heavy prongs per star $\langle \Sigma T_H \rangle$ is 132 MeV. (No binding energy is included.) The corresponding distribution for antiproton stars [16] with $\langle \Sigma T_H \rangle = 147$ MeV is also shown in the figure. Use has already been made of the close similarity of the two distributions in the discussion in section 4.1.

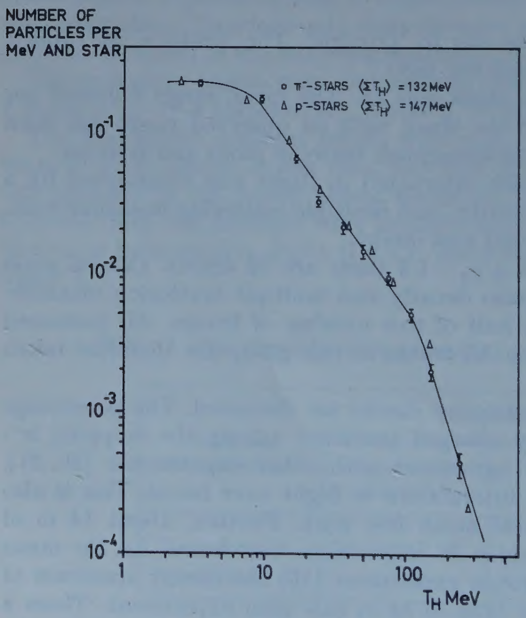

Fig. 5.

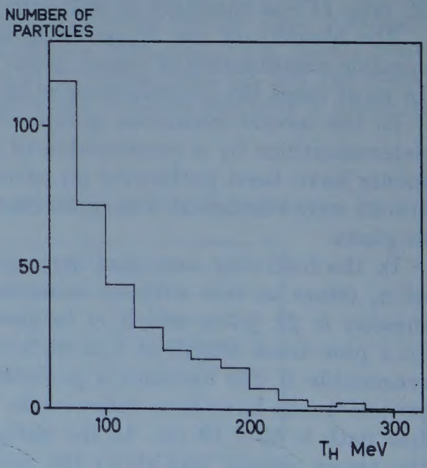

Fig. 6.

Fig. 5. The number of heavy prongs per star and MeV from pion stars (dots) and antiproton stars (triangles) as a function of the kinetic energy of the particle.

Fig. 6. The energy distribution of protons with kinetic energy above 60 MeV.

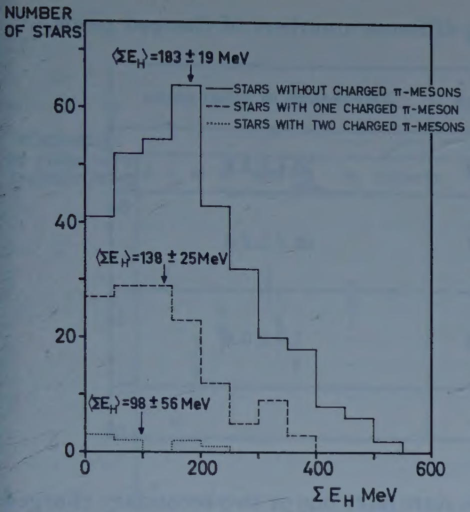

Fig. 7.

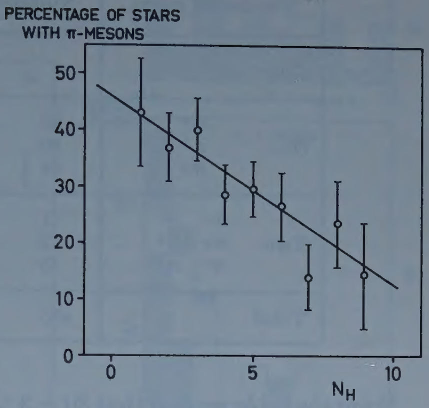

Fig. 8.

Fig. 7. The distributions of the visible energy seen in heavy prongs per star.

Fig. 8. The percentage of stars with charged pions as a function of the emitted number of charged heavy particles.

The high energy part, above 60 MeV, of the distribution in Fig. 5 is shown in Fig. 6. This does not agree with the spectrum measured by Blau and Caulton at 500 MeV [8]. They find that about 8 % of the protons with T_H above 60 MeV have T_H above 280 MeV. We have one case out of 325.

The distributions of the visible energy in heavy prongs per star are shown in Fig. 7. The mean values, $\langle \Sigma E_H \rangle$, are, for stars with no charged pion 183 ± 19 MeV, for stars with one charged pion 138 ± 25 MeV, and for stars with two charged pions 98 ± 56 MeV. A binding energy of 8 MeV is included.

We will now discuss the heavy prong distributions (Fig. 4) somewhat more. These distributions are certainly biassed. Stars with no heavy prong and a number of stars with one heavy prong will be overlooked in area scanning. An unbiassed heavy prong distribution from antiproton stars is given in reference [16], where $\langle N_H \rangle = 4.51$. This is about the same as $\langle N_H \rangle$ in the present experiment. We will make use of the fact that the number of one- and two-prong stars is about the same in the antiproton case, to infer that it should be the same even in the present case. This means that the number of one heavy prong stars should be corrected by about 50 %. Blau and Caulton [8] have investigated the scanning efficiency of finding one heavy prong star and have obtained the value 50 ± 10 %.

We will not try to estimate the number of stars with zero black prongs because of the large uncertainties.

4.3 *Frequencies of charged pions*

In Table 2 the stars are divided into phenomenological groups according to the observed number of pions and their charges.

Table 2. Frequencies of stars containing different numbers of charged pions.

Number of pions		Number of stars		Percentage of total cases
Zero			340	70.1 ± 3.8
One	π^-	39	137	28.2 ± 2.4
	π^+	10		
	$\pi^\pm$	88		
Two	π^- π^-	1	8	1.7 ± 0.6
	π^+ $\pi^\pm$	2		
	π^- $\pi^\pm$	5		
Total		485		

From the table we find that 30 ± 3 % of the stars have one or two secondary charged pions. This figure is, however, slightly biassed, which is seen from the following facts.

(i) We know from an earlier experiment [16] under identical conditions that the scanning efficiency of finding tracks with $g/g_0 < 1.4$ is about 90 % when the stars have been looked upon once in order to decide if there is a track of low ionization or not. 92 such π-mesons have been seen so we can estimate having missed about 10.

(ii) The type of stars picked up by area scanning is biassed. All stars with no black prong and a number of stars with one black prong will be overlooked. The effect of this bias can be seen in Fig. 8. The percentage of stars with charged pions is plotted against the number of heavy prongs in the star. Stars with few heavy prongs contain relatively more charged pions.

We assume that there is no bias in picking up stars with $N_H \geqslant 2$ and that the number of one-prong stars should be corrected by 50 % (section 4.2).

We can now by means of (i) and (ii) deduce a corrected percentage of stars with charged pions of 33 ± 4 %.

This figure is very insensitive to the correction for one-prong stars.

Only a large fraction of zero heavy prong stars could raise this fraction appreciably. That the fraction of stars with no heavy prong is large is indicated by the heavy prong distribution of antiproton stars [16] and by π-meson experiments at 750 MeV [9]. If we assume the fraction of zero prong stars to be 20 %, the percentage of stars with charged pions will be 36.

The results of different emulsion experiments [1–11] and a Monte Carlo calculation for Ru^{100} by Metropolis *et al.* [22], as regards the percentage of stars with charged pions, is shown in Fig. 9. Our result fits, within the errors, into the picture.

5. Analysis of stars with one negative secondary pion

5.1 *Angular distribution*

It will be assumed that the pion interacts with one or two nucleons in the primary process in the nucleus. The following one-nucleon processes with emission of one or two pions are possible.

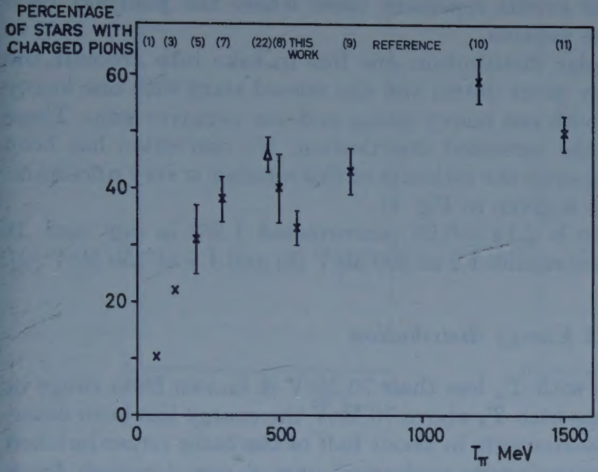

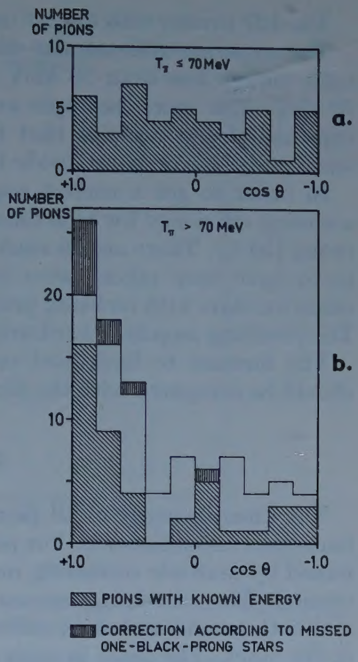

Fig. 9.

Fig. 10.

Fig. 9. Fraction of stars with charged secondary pions as a function of the kinetic energy of the incident pion.

Fig. 10. Angular distribution of pions from stars with one negative pion.

$$\begin{aligned}
\pi^- + p &\rightarrow \pi^- + p && (a)\\
&\rightarrow \pi^0 + n && (b)\\
&\rightarrow \pi^- + \pi^0 + p && (c)\\
&\rightarrow \pi^- + \pi^+ + n && (d)\\
&\rightarrow \pi^0 + \pi^0 + n && (e)\\
\pi^- + n &\rightarrow \pi^- + n && (f)\\
&\rightarrow \pi^- + \pi^0 + n && (g)\\
&\rightarrow \pi^- + \pi^- + p && (h)
\end{aligned}$$

Pion production will be treated in section 7. It constitutes only a small fraction of the total number of reactions. Stars with one π^+ arise from the process (d) or from charge exchange of a secondary neutral pion: $\pi^0 + p \rightarrow \pi^+ + n$. The energy distribution of the positive pions (Table 4) drops sharply above 50 MeV. It is almost unbiassed up to 70 MeV, as only two pions with kinetic energy less than this limit leave the stack (Table 1). We therefore think that most of the positive pions have been identified. Of the events in Table 2, the stars with one $\pi^\pm$ (88) and one π^- (39) are thus mainly due to the reactions (a) and (f). The contamination of events with pion production and charge exchange scattering twice can be neglected.

The 127 events with one $\pi^\pm$ or one π^- are treated in this section.

The experimental angular distribution is given in Fig. 10*a*, for the pions with kinetic energy less than 70 MeV and Fig. 10*b*, for the pions with kinetic energy above 70 MeV. The more isotropic angular distribution of the low energy pions can be expected if one assumes that the events represent cases where the pion has been scattered twice or more inside the nucleus.

In order to get a correct angular distribution one has to take into account the scanning efficiency for high energy pions (90 %) and the missed stars with one heavy prong (50 %). There are 10 stars with one heavy prong and one negative pion. These pions have been taken twice in the corrected distribution. No correction has been made for stars with no black prong since the estimate of this number is very uncertain. The resulting angular distribution is given in Fig. 11.

The forward to backward ratio is 2.14 ± 0.20 (uncorrected 1.95) in our case. It should be compared with the earlier results 1.2 at 500 MeV [8] and 1.7 at 750 MeV [9].

5.2 *Energy distribution*

The kinetic energy of all pions with T_π less than 70 MeV is known from range or ionization measurements. For pions with T_π above 70 MeV the energy has been determined by multiple scattering measurements in about half of the cases (cross-hatched events). The scattering measurements were performed over 6 mm for each track and both second and third differences were calculated. The distortion was very small in the stack. The error in each energy determination is about ± 15 %.

We find a marked relation between the energy and the angle of emission. The data are given in Table 3.

Table 3. The kinetic energy of pions for different space-angle intervals.

$\cos\theta$ interval	Pions with $g/g_0 < 1.4$		All pions Average kinetic energy (MeV)
	Number of pions measured	Average kinetic energy (MeV)	
$+1.0 \rightarrow +0.8$	16	298 ± 32	252 ± 32
$+0.8 \rightarrow +0.4$	12	248 ± 47	200 ± 40
$+0.4 \rightarrow -1.0$	15	179 ± 23	121 ± 18

Belovitskii [7] has found the same effect for negative pion stars at 300 MeV, whereas Blau and Caulton [8] find only a slight correlation at 500 MeV. The correlation can be expected because of the movement of the center-of-momentum.

In order to get an unbiassed energy distribution of the pions we have proceeded in the following way.

(i) The pions whose energies have not been measured are assumed to have the same energy distribution as the measured pions in the same space angle interval.

(ii) The high energy part of the spectrum $T_\pi > 70$ MeV has been enlarged by a factor 1/0.9 arising from the detection efficiency for high energy pions.

(iii) The scanning bias for stars with one black prong (50 %) has been taken into account as explained in the preceding section.

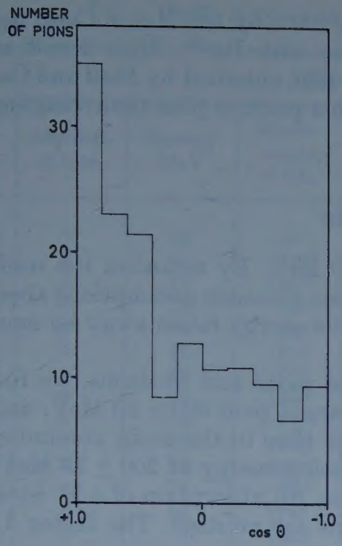

Fig. 11.

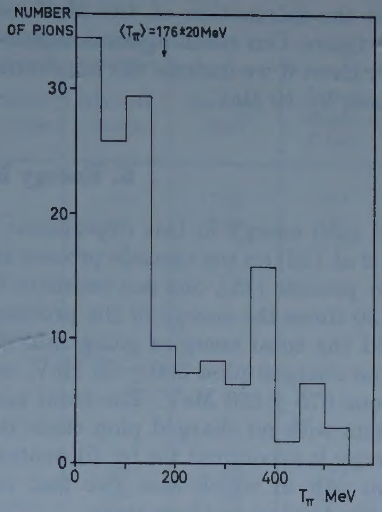

Fig. 12.

Fig. 11. Total angular distribution of pions from stars with one negative pion corrected for scanning losses of minimum tracks and one-heavy-prong stars.

Fig. 12. Energy distribution of pions from stars with one negative pion.

The pions in Fig. 10*a* and *b*, will then give the corrected energy distribution (Fig. 12). The peak at 350–400 MeV is not significant, since it is based only on seven measured tracks.

The average kinetic energy of the secondary pions is 176 ± 20 MeV. This result is probably a lower limit, since we have excluded stars with no heavy prongs and these stars are likely to contain a high energy pion.

The experimental results on the average kinetic energy of the inelastically scattered pions at different energies of the incident pion, obtained by different laborato-

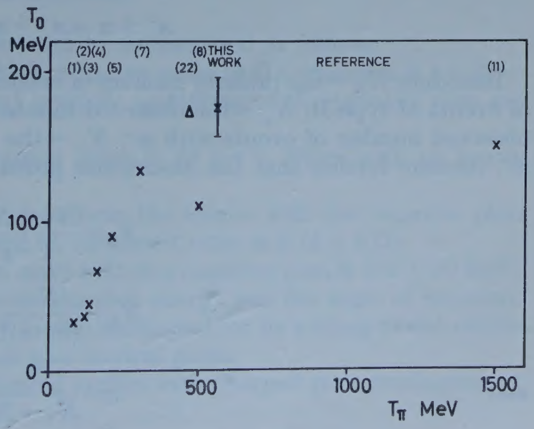

Fig. 13. The average kinetic energy (T_0) of inelastically scattered negative pions as a function of the kinetic energy (T_π) of the incident pion.

ries, are collected in Fig. 13. Metropolis *et al.* [21] have by the Monte Carlo method investigated the interaction of 465 MeV π-mesons with Ru^{100}. Their result is also given in the figure. Our result again disagrees with that obtained by Blau and Caulton at 500 MeV. Even if we include the ten events with a positive pion the average energy only decreases by 10 MeV.

6. Energy balance

The total pion energy in this experiment is 700 MeV. By means of the results of Metropolis *et al.* [22] on the cascade process and some plausible assumptions about the evaporation process [15], one can estimate that the energy taken away by neutrons is 1.75 ± 0.30 times the energy of the protons.

If we add the total energies going into charged pions and nucleons, we find for stars with no charged pion 500 ± 75 MeV, one charged pion 690 ± 80 MeV, and two charged pions 675 ± 150 MeV. The total energy is thus in the main accounted for.

In the stars with no charged pion there is a missing energy of 200 ± 75 MeV. The missing energy is accounted for by (i) neutral pions, (ii) absorption of a π^- by a proton–neutron pair in which case two fast neutrons are emitted. The factor 1.75 is then probably too low in these stars.

7. Pion production

The events with two charged pions arising from pion production and the events with one positive pion representing possible pion production are listed in Table 4. The kinetic energy, space angle with respect to the primary pion and terminal behaviour of the pions are given. We first notice the energy distribution of the π^+-mesons which drops sharply above 50 MeV. This makes it very likely, as has been pointed out before, that the π^+ energy distribution is fairly unbiassed.

If we restrict ourselves to pion production in one-nucleon reactions the possible types of reactions are given by the relations (*c*), (*d*), (*e*), (*g*) and (*h*) (section 5.1). We choose to investigate production of one charged pion, i.e.

$$\pi^- + p \rightarrow \pi^- + \pi^+ + n \tag{A}$$

$$\pi^- + n \rightarrow \pi^- + \pi^- + p \tag{B}$$

Introduce N_A = the primary number of events of type A, N_B = the primary number of events of type B, $N_\pm$ = the observed number of events with π^+ and π^-, N_+ = the observed number of events with π^+, $N_=$ = the observed number of events with two π^-. Assume further that the absorption probability of a secondary pion is ε. Then

$$N_A = \frac{N_+ + N_\pm}{1-\varepsilon},$$

$$N_B = \frac{N_=}{(1-\varepsilon)^2},$$

and

$$\varepsilon = \frac{N_+}{N_+ + N_\pm}.$$

Table 4. Events with charged pion production.

Event no.	Characteristics of emitted pions							
	Identification	Energy MeV	Space-angle, θ lab.	Terminal behaviour	Identification	Energy, MeV	Space-angle, θ lab.	Terminal behaviour
129	π^+	38	85°	Decays at rest	$\pi^\pm$	104	57°	Leaves stack
3128	π^+	41	67°		$\pi^\pm$	330	51°	
4	π^+	41	121°					
88	π^+	79	85°					
89	π^+	48	35°					
1026	π^+	46	47°					
1066	π^+	48	67°					
2006	π^+	34	130°					
2009	π^+	24	41°					
2012	π^+	58	123°					
2058	π^+	23	138°					
3068	π^+	27	75°					
1008	π^-	52	114°	Absorption star, at rest	π^-	56	43°	π_ϱ
65	π^-	8	103°		$\pi^\pm$	68	59°	Leaves stack
2043	π^-	38	62°		$\pi^\pm$	104	68°	
2065	π^-	42	50°		$\pi^\pm$	60	94°	
3022	π^-	50	123°		$\pi^\pm$	89	52°	
3037	π^-	40	142°		$\pi^\pm$	85	97°	

Among the events with one positive pion, we estimate that the number which arises from double charge-exchange scattering is of the same order as the number which comes from pion production. It is assumed that the scattering proceeds through the isospin $T = 3/2$ channel in this estimate. Of the five events with π^- and π^+, two are taken as $(\pi^-\pi^-)$ and three as $(\pi^-\pi^+)$. With $N_+ = 5$ (half of the total number), $N_\pm = 5$ and $N_= = 3$, we find $N = N_A + N_B = 32 \pm 20$. Thus the percentage of events with charged pion production is $7 \pm 4\,\%$.

8. Conclusions

The results of the present experiment can be summarized as follows.

(i) The total mean free path of 560 MeV negative pions in G5 emulsion is $\lambda = 28 \pm 2$ cm. Absorption, charge exchange and inelastic scattering of the primary pion are included in this mean free path.

(ii) The frequency of stars with charged pions is $33 \pm 4\,\%$. Stars with no heavy prong are excluded in this estimate.

(iii) The angular distribution of the pions from the events with one negative pion is strongly peaked forward. The forward to backward ratio is 2.14 ± 0.20.

(iv) The average energy of pions from stars with one negative pion is 176 ± 20 MeV.

(v) A marked correlation exists between the pion energy and the angle of emission.

(vi) The total pion energy of 700 MeV is well accounted for by adding to the visible energy the energy taken up by neutrons and neutral pions.

(vii) A rough estimate gives a fraction of events with charged pion production of $7 \pm 4\,\%$.

ACKNOWLEDGEMENTS

We express our deep gratitude to the Bevatron group and its head, Dr. E. J. Lofgren, and to Professor A. G. Ekspong for exposing the stack and helping in planning the experiment.

The facilities put at our disposal by Professor Kai Siegbahn are gratefully acknowledged as is his continued interest in this work.

We thank our scanners Mrs. S. Eklund, Miss B. Lundkvist, Miss I. Durén, Miss M. Pearce, Miss M. Källsten, and Miss B. Comstedt for their excellent work.

The research was partly sponsored by the Air Research and Development Command through its European Office. Support was also obtained from the Swedish Atomic Research Council.

One of us (W.S.) would like to thank the Swedish Institute for financial support.

Institute of Physics, University of Uppsala, Uppsala, Sweden.

REFERENCES

1. Bernardini, G., Booth, E. T., Lederman, L., and Tinlot, J., Phys. Rev. *80*, 924 (1950) and *82*, 105 (1951).
2. Ferrari, G., Ferretti, L., Gessaroli, R., Manaresi, E., Pedretti, E., Puppi, G., Quareni, G., Ranzi, A., Stranghellini, A., and Stantic, S., Nuovo Cimento Suppl. *4*, 914 (1956).
3. Goldhaber, G., and Goldhaber, S., Phys. Rev. *91*, 467 (1953).
4. Nikolskii, B. A., Kudrin, L. P., and Ali-Zade, S. A., Soviet Phys. JETP *5*, 93 (1957).
5. Morrish, A. H., Phys. Rev. *90*, 674 (1953) and Phil. Mag. *45*, 47 (1954).
6. Fry, W. F., Phys. Rev. *91*, 1576 (1953).
7. Belovitskii, G. E., Soviet Phys. JETP *8*, 581 (1959).
8. Blau, M., and Caulton, M., Phys. Rev. *96*, 150 (1954).
9. Blau, M., and Oliver, A. R., Phys. Rev. *102*, 489 (1956).
10. Blau, M., Carter, C. F., and Perlmutter, A., Nuovo Cimento *4*, 704 (1959).
11. Crew, J. E., and Hill, R. D., Phys. Rev. *110*, 177 (1958).
12. Walker, W. D., and Crussard, J., Phys. Rev. *98*, 1416 (1955).
13. Walker, W. D., Hushfar, F., and Shephard, W. D., Phys. Rev. *104*, 526 (1956).
14. Hill, R. D., Salant, E. O., Widgoff, M., Osborne, L. S., Pevsner, A., Ritson, D. M., Crussard, J., and Walker, W. D., Phys. Rev. *101*, 1127 (1956).
15. Chamberlain, O., Goldhaber, G., Jauneau, L., Kalogeropoulos, T., Segrè, E., and Silberberg, R., Phys. Rev. *113*, 1615 (1959).
16. Ekspong, A. G., Frisk, Å., Nilsson, S., and Ronne, B. E., Nuclear Physics (to be published).
17. Barbaro, A., Baroni, G., and Castagnoli, C., Nuovo Cimento *9*, 154 (1958) and private communication.
18. Ekspong, A. G., Johansson, S., and Ronne, B. E., Nuovo Cimento *8*, 84 (1958).
19. Rossi, B., and Greisen, K., Rev. Mod. Phys. *13*, 240 (1941).
20. Adelman, F. L., and Jones, S. B., Phys. Rev. *75*, 1468 (1949).
21. Menon, M. G. K., Muirhead, H., and Rochat, O., Phil. Mag. *41*, 583 (1950).
22. Metropolis, N., Bivins, R., Storm, M., Miller, J. M., Friedlander, G., and Turkevich, A., Phys. Rev. *110*, 204 (1958).

Tryckt den 30 januari 1961

Uppsala 1961. Almqvist & Wiksells Boktryckeri AB